

POLARIZATION TRANSFER IN ELASTIC ELECTRON SCATTERING  
FROM NUCLEONS AND DEUTERONS\*

Raymond G. Arnold<sup>†</sup>

The American University  
Washington, D.C. 20016

Carl E. Carlson and Franz Gross

Department of Physics  
College of William & Mary  
Williamsburg, Virginia 23185

ABSTRACT

We present a description, including relevant formulas and numerical estimates, of a set of polarization transfer experiments which appear to offer a feasible way to a) separate the deuteron charge and quadrupole form factors and b) measure the neutron and proton electric form factors. The experiments require a 2 to 4 GeV high-intensity, high-duty factor, longitudinally polarized electron beam, and require that the polarization of the recoiling hadron be measured in a second, analyzing, scattering. The relevant asymmetries are fairly large, and our calculations show that they are sensitive to different models obtained from existing data. Attention is called to the fact that the proposed deuteron measurements will require new 10% measurements of vector and tensor analyzing powers of deuterons with kinetic energy from 150 to 450 MeV.

(Submitted to Phys. Rev. C)

---

\*Work supported in part by the Department of Energy, contract DE-AC03-76SF00515 and by the National Science Foundation Grants PHY78-09378 and PHY79-19071.

<sup>†</sup>Permanent Address: Stanford Linear Accelerator Center  
Stanford University, Stanford, California 94305

## I. OVERVIEW AND SUMMARY

### A. Introduction

A complete understanding of the electromagnetic structure of the neutron and proton requires knowledge of both the electric form factors ( $G_{En}$  and  $G_{Ep}$ ) and the magnetic form factors ( $G_{Mn}$  and  $G_{Mp}$ ); yet in the region of four-momentum transfer squared,  $Q^2$ , greater than  $2 \text{ (GeV/c)}^2$  the electric form factors are very poorly known. The situation for the deuteron is even worse; there we need to know three form factors, the charge,  $G_C$ , quadrupole,  $G_Q$ , and the magnetic,  $G_M$ , but only one combination of these,  $A = G_C^2 + \frac{8}{9}\eta^2 G_Q^2 + \frac{2}{3}\eta G_M^2$  is known for  $Q^2 > 1 \text{ (GeV/c)}^2$ . If we could separately determine all of the nucleon and deuteron form factors, our knowledge of the physics of these systems would be greatly increased. In this paper we will report calculations, and suggest experiments which appear to offer a feasible way to do this. A key factor in these experiments is the use of longitudinally polarized electron beams.

Electron beams with 85% polarization and low intensity<sup>1</sup> and 40% polarization and high intensity<sup>2</sup> have been used at SLAC, and there is hope that beams which are both highly polarized and intense will be available in the near future.<sup>3</sup> Such beams can be used to separate the form factors, provided the polarization of either the initial or final hadron is also known. While polarized targets have already been used with low-intensity beams,<sup>1</sup> there appear to be fundamental difficulties in using them with the high-intensity beams required for measurements at high  $Q^2$  where the counting rates are low. It is therefore natural to examine the alternative where polarization of the recoiling hadron is measured by looking at the asymmetry produced in a second scattering. Such a detector (polarimeter)

will inevitably have low efficiency ( $10^{-3}$  to  $10^{-5}$ ), but has advantages over a polarized target in that it would be a relatively simple, passive system with little or no dead time, can analyze many states for which polarized targets are not available, and can take full advantage of the high current and high duty factor planned for the next generation of electron accelerators.

To extract the form factors to 10% accuracy from the asymmetries measured in the second scattering requires that the analyzing powers of the second scattering should also be known to at least 10% accuracy. Analyzing powers for neutrons and protons have already been measured<sup>4</sup> at the right energies and to the required level of accuracy. Better measurements of these would be desirable, but are not essential. For the deuteron the situation is less favorable. Analyzing powers are known only for a few selected targets at a few isolated energies and scattering angles. Both the vector and tensor powers have been measured<sup>5</sup> at 420 MeV deuteron lab energy (corresponding to  $Q^2$  of  $1.6 \text{ (GeV/c)}^2$ ), and while some vector power measurements have been made at lower energies<sup>6</sup> (94-157 MeV corresponding to  $Q^2$  of 0.35 to  $0.6 \text{ (GeV/c)}^2$ ), the tensor powers were not observed there. New, 10% measurements of all the analyzing powers from 150 to 450 MeV are needed before the experiments outlined in part B below can be carried out to the 10% accuracy desired, and more nuclei should be searched to find those which give particularly large analyzing powers.

The asymmetries expected for the experiments proposed in this paper are typically of the order of 0.10, so that while the experiments will be difficult, it should be feasible to measure these to the desired 10% accuracy. We also wish to point out at the outset that, while most of the

measurements discussed in this paper require longitudinally polarized electron beams, some of the measurements for the deuteron are possible without polarized beams.

We turn now to a discussion of the proposed experiments. Since the detailed considerations are different, the deuteron, neutron, and proton will be discussed in separate parts below. Finally, some details of the calculations for the deuteron are given in Section II.

### B. Deuteron

Three form factors —  $G_C$ ,  $G_M$ , and  $G_Q$  for the charge, magnetic moment, and quadrupole moment distributions — describe the electromagnetic interaction of the deuteron in elastic scattering. These form factors depend directly on the wave function of the deuteron. Measuring the three deuteron form factors is thus a test of our knowledge of the nucleon-nucleon interaction; at higher momentum transfers where relativistic corrections or meson exchange currents become important our understanding of these matters is also probed. The deuteron form factors are proportional to the electromagnetic form factors of the constituent nucleons and at high  $Q^2$  uncertainties in (particularly) the neutron form factors presently hamper our ability to extract information dependent only on the nucleon interaction.

In scattering unpolarized electrons from unpolarized deuterons, only two combinations of the three form factors can be separated. The differential cross section is given by

$$\frac{d\sigma}{d\Omega} = \frac{d\sigma}{d\Omega} \Big|_{NS} \left[ A + B \tan^2 \left( \frac{1}{2} \theta \right) \right] \quad (1)$$

where  $\theta$  is the lab scattering angle of the electron,  $d\sigma/d\Omega \Big|_{NS}$  is the cross section for structureless particles,

$$\frac{d\sigma}{d\Omega} \Big|_{NS} = \left(\frac{\alpha}{2E}\right)^2 \frac{\cos^2\left(\frac{1}{2}\theta\right)}{\sin^4\left(\frac{1}{2}\theta\right)} \frac{1}{\left(1 + \frac{2E}{M_d} \sin^2\left(\frac{1}{2}\theta\right)\right)} \quad (2)$$

and

$$A = G_C^2 + \frac{2}{3}\eta G_M^2 + \frac{8}{9}\eta^2 G_Q^2$$

$$B = \frac{4}{3}\eta(1+\eta) G_M^2 \quad (3)$$

$$\eta = \frac{Q^2}{4M_d^2}$$

where  $Q^2$  is the four momentum transfer squared. (Our conventions follow Bjorken and Drell, and if  $Q$  is the momentum transfer,  $Q^2 \equiv -q^2 > 0$ .) Accurate measurements over a range of angles can determine  $G_M$ , but cannot separate  $G_C$  from  $G_Q$ .

To aid in separating  $G_C$  from  $G_Q$ , we discuss polarization experiments. In particular, consider scattering longitudinally polarized electrons from unpolarized deuterons.<sup>7</sup> The outgoing deuteron from this reaction will have vector and tensor polarizations  $p_i$  and  $p_{ij}$  ( $i, j = x, y, z$ ) which can be calculated in terms of the three deuteron form factors and which can be measured by a second, analyzing, scattering from another (perhaps carbon) target. The cross section for the two scatterings together in the coordinate systems of Fig. 1, is<sup>8</sup>

$$\begin{aligned} \frac{d\sigma}{d\Omega d\Omega_2} = \frac{d\sigma}{d\Omega d\Omega_2} \Big|_0 \left\{ 1 + \frac{3}{2} a p_x A_y \sin\phi_2 + \frac{1}{2} p_{zz} A_{zz} \right. \\ \left. + \frac{2}{3} p_{xz} A_{xz} \cos\phi_2 \right. \\ \left. + \frac{1}{6} (p_{xx} - p_{yy})(A_{xx} - A_{yy}) \cos 2\phi_2 \right\} \end{aligned} \quad (4)$$

Here,  $a$  is the polarization of the incoming electron beam (i.e.,  $a$  is the probability of finding a right-handed polarized electron minus the

probability of finding a left-handed one;  $|a| \leq 1$ ). The quantity  $\frac{d\sigma}{d\Omega d\Omega_2} \Big|_0$  is the cross section for scattering with unpolarized electrons followed by a second scattering with unpolarized deuterons. The azimuth angle between the two scattering planes is  $\phi_2$  (see Fig. 1). The only  $\phi_2$  dependence is in the sines and cosines displayed explicitly above, so that a simple Fourier analysis will separate all the terms except  $p_{zz}$ . The second scattering has analyzing powers  $A_i$  and  $A_{ij}$  which are functions of the energy of the deuteron which enters the second scattering and of the second scattering angle  $\theta_2$ . We could also say that they were functions of  $Q^2$  and  $\theta_2$  since the kinetic energy of the deuteron entering the second scattering is given by

$$K' = \frac{Q^2}{2M_d} \quad (5)$$

The values of  $A_i$  and  $A_{ij}$  must be measured in a separate experiment.

The non-zero polarizations are given in terms of  $Q^2$ ,  $\theta$ ,  $G_C(Q^2)$ ,  $G_M(Q^2)$ , and  $G_Q(Q^2)$  by

$$\begin{aligned} I_0 p_x &= -\frac{4}{3} \sqrt{\eta(1+\eta)} G_M \left( G_C + \frac{1}{3} \eta G_Q \right) \tan\left(\frac{1}{2}\theta\right) \\ I_0 p_z &= \frac{2}{3} \eta \sqrt{(1+\eta) \left(1 + \eta \sin^2\left(\frac{1}{2}\theta\right)\right)} G_M^2 \tan\left(\frac{1}{2}\theta\right) \sec\left(\frac{1}{2}\theta\right) \\ -I_0 p_{zz} &= \frac{8}{3} \eta G_C G_Q + \frac{8}{9} \eta^2 G_Q^2 + \frac{1}{3} \eta \left(1 + 2(1+\eta) \tan^2\left(\frac{1}{2}\theta\right)\right) G_M^2 \\ I_0 (p_{xx} - p_{yy}) &= -\eta G_M^2 \\ I_0 p_{xz} &= -2\eta \sqrt{\eta + \eta^2 \sin^2\left(\frac{1}{2}\theta\right)} G_M G_Q \sec\left(\frac{1}{2}\theta\right) \end{aligned} \quad (6)$$

where

$$I_0 = A + B \tan^2\left(\frac{1}{2}\theta\right) \quad (7)$$

and some readers may wish to rewrite two of the above using

$$\sqrt{\eta + \eta^2 \sin^2\left(\frac{1}{2}\theta\right)} = \frac{E + E'}{2M_d} \sin\left(\frac{1}{2}\theta\right) \quad (8)$$

where  $E$  and  $E'$  are the initial and final electron lab energies. We give  $p_z$  even though it does not enter the cross section Eq. (4) directly. In practice, the deuteron may pass through a magnetic field between the first and second scattering, causing the polarizations to precess. Then in order to calculate the vector polarization components of the deuteron when it enters the second reaction, both  $p_x$  and  $p_z$  of the deuteron as it emerges from the first reaction must be known.

Polarizations  $p_x$  and  $p_{xz}$  are the most interesting because they involve combinations of  $G_C$  and  $G_Q$  different from  $A(Q^2)$ . Polarization ( $p_{xx} - p_{yy}$ ) is less interesting from this viewpoint since it depends only on  $G_M^2$ , which could be measured with no polarization analysis. Also we shall see that ( $p_{xx} - p_{yy}$ ) gives contributions in Eq. (4) that are numerically small. If the absolute normalization of an experiment proves hard to determine, then the only quantities that come easily from a Fourier analysis in  $\phi_2$  are the ratios  $p_x/p_{xz}$ ,  $p_x/(1 + \frac{1}{2}p_{zz} A_{zz})$ , and  $p_{xz}/(1 + \frac{1}{2}p_{zz} A_{zz})$ . If the initial electrons are unpolarized, only the last ratio can be measured. The last two ratios can determine  $p_x$  and  $p_{xz}$  individually only if we have separate information about  $p_{zz}$ . In some cases one might be willing to trust a calculation of  $p_{zz}$ : it can happen that the uncertainty or model dependence of  $p_{zz}$  is large but that this does not cause a large percentage uncertainty in  $(1 + \frac{1}{2}p_{zz} A_{zz})$ . However, the first ratio yields:

$$\frac{p_x}{p_{xz}} = \frac{4}{3} \sqrt{\eta(1+\eta)} \frac{M_d}{E + E'} \left( \frac{G_C}{\eta G_Q} + \frac{1}{3} \right), \quad (9)$$

which gives new information and can be determined independently of  $p_{zz}$  and  $G_M$ .

A few remarks should be made regarding why the particular polarizations in Eq. 6 are non-zero. If neither of the initial particles were polarized, parity invariance could be used to show that  $p_x = p_z = 0$ . In the present case, this does not apply, and neither  $p_x$  nor  $p_z$  is zero. In general  $p_y$  is not zero. It is not forbidden by parity or any other invariance principle. That  $p_y = 0$  here is a consequence of making the usual one-photon-exchange approximation. Also with the one-photon-exchange approximation, the tensor polarizations are independent of the electron polarization. Hence only the tensor polarizations which would be present if the initial particles were not polarized, i.e., those tensor polarizations allowed by parity invariance, are non-zero. These are  $p_{zz}$ ,  $p_{xz}$ , and  $(p_{xx} - p_{yy})$ , and they could be measured without having a polarized electron beam.

To our knowledge, the formulas for the vector polarization are new. The tensor polarizations have been discussed before.<sup>9</sup> The component  $p_{zz}$  is the same as  $-\sqrt{2} T_{20}$ , where  $T_{20}$  is the tensor polarization studied by Levinger et al.<sup>10</sup> and by Moravcsik and Ghosh.<sup>11</sup> (The formula for  $T_{20}$  is sometimes quoted after doing an extrapolation in  $\theta$  to remove the  $G_M^2$  terms.) The other tensor polarizations  $p_{xz} = -\sqrt{3} T_{21}$  and  $(p_{xx} - p_{yy}) = 2\sqrt{3} T_{22}$  have been recently studied by Haftel, Mathelitsch, and Zingl,<sup>12</sup> who examined the sensitivity to different deuteron wave functions.

We have calculated the polarizations over a range of angle and  $Q^2$  for several different deuteron wave functions. Our calculations of  $G_E$ ,  $G_M$ , and  $G_Q$  follow Ref. 13, so that we have a fully relativistic calculation of the impulse approximation. This means that some corrections sometimes counted among meson exchange corrections, namely the pair currents,<sup>14</sup> are automatically included, although true meson exchange corrections such as

the photon coupling to a  $\rho$ - $\pi$  current are not. The three deuteron form factors depend on the nucleon electromagnetic form factors as well as on the deuteron wave function. Our plots are all prepared using the nucleon form factors called "Best Fit" in Ref. 13.

Results of our calculation for the deuteron are shown in Figs. 2 through 4. Figure 2 displays the five non-zero polarizations vs. scattering angle for several values of  $Q^2$  and one wave function, namely the HM3 wave function from the Bonn group.<sup>15</sup> Polarization  $p_{xz}$  is large at most angles (so we should measure it where the event rate is high) and changes sign at a particular  $Q^2$  whose value we shall see is model sensitive. Polarization  $p_x$  is larger for backward scattering, where the event rate is small, than it is for forward scattering, where the event rate is large. If one considers only statistical errors, the figure of merit for a measurement is proportional to the (event rate)<sup>1/2</sup>  $\times$  (polarization), and for  $p_x$  this number is not strongly angle dependent and in fact slightly favors forward directions. Hence one may expect that experiments will be done at forward angles. To reduce clutter on our graphs when we consider different deuteron wave functions, we shall fix  $\theta$  at a moderately forward angle like  $40^\circ$ .

In Fig. 3 we show the five polarizations vs.  $Q^2$  for a number of deuteron wave functions at  $\theta = 40^\circ$ . Results from the Reid soft core<sup>16</sup> wave function with the form factors calculated non-relativistically have been included as a benchmark. We then show results from four credible model wave functions calculated relativistically. These are the Reid soft core wave function, the HM3 wave function,<sup>15</sup> the Lomon-Feshbach wave function with 4.57% D-state<sup>17</sup> and the  $\lambda = 0.4$  member of a family of relativistic wave

functions.<sup>18</sup> The Lomon-Feshbach wave function is quite interesting in that it fits the deuteron parameters, and the potential that generates it fits the phase shifts well, but the results it gives for the quantities of interest here are rather different from the other wave functions. Note that measurements with 10% errors are sufficient to distinguish the models from each other.

The ratio  $p_x/p_{xz}$  appears in Fig. 4 for  $\theta = 40^\circ$  and the same deuteron models as in Fig. 3. The model sensitive point where  $p_x/p_{xz}$  is zero is due to, although somewhat displaced from, the zero and associated sign change of  $G_C$  at  $Q^2 \leq 1 (\text{GeV}/c)^2$ . Polarizations  $p_x$  and  $p_{xz}$  individually also have zeros at  $Q^2$  of 1.4 to 1.6  $(\text{GeV}/c)^2$  due to  $G_M$ , but these cancel in the ratio. Since  $G_C$  and  $G_Q$  depend primarily on the isoscalar electric nucleon form factor (and not the magnetic), the ratio  $p_x/p_{xz}$  is insensitive to the nucleon form factor model.

There is a need for more experimental measurements of the analyzing powers  $A_y$ ,  $A_{zz}$ ,  $A_{xz}$  and  $(A_{xx} - A_{yy})$  at energies of interest here (deuteron lab energies 150 to 450 MeV). Some data do already exist.<sup>5,6</sup> For  $Q^2 = 1.6 (\text{GeV}/c)^2$  we can use the analyzing powers reported in Ref. 5, taking  $\theta_2 = 6^\circ$  to  $10^\circ$  for definiteness, to estimate the size of effects that can be obtained for various electron scattering angles  $\theta$ . For example, taking  $\theta = 40^\circ$  and  $p_i$  and  $p_{ij}$  from the Lomon-Feshbach wave function, we get

$$\left\{ \begin{aligned} &1 + \frac{3}{2} a p_x A_y \sin\phi_2 + \frac{1}{2} p_{zz} A_{zz} \\ &+ \frac{2}{3} p_{xz} A_{xz} \cos\phi_2 \\ &+ \frac{1}{6} (p_{xx} - p_{yy})(A_{xx} - A_{yy}) \cos 2\phi_2 \end{aligned} \right\} \approx \left\{ \begin{aligned} &1 - 0.1 a \sin\phi_2 - 0.23 \\ &- 0.88 \cos\phi_2 - 0.01 \cos 2\phi_2 \end{aligned} \right\} \quad (10)$$

Effects from  $(p_{xx} - p_{yy})$  are small. However, the amplitude of the sinusoidal variation is not small, and a good determination of its phase as well as its amplitude will yield both  $p_x$  and  $p_{xz}$ .

### C. The Neutron

The goal is to learn about the neutron form factors. They are in general difficult to measure because there are no free neutron targets and recoil neutrons are difficult to detect. The magnetic form factor  $G_{Mn}$  is the best known because it is relatively large and can be determined from the slope in the Rosenbluth plots of cross section vs. electron scattering angle; it has been measured<sup>19</sup> up to  $Q^2$  of  $2.7 \text{ (GeV/c)}^2$  in quasi-free electron-deuteron scattering with uncertainties ranging from 10% to 40%. The electric form factor  $G_{En}$  is very small, and therefore is generally very poorly known, except for the slope at  $Q^2 = 0$ , which has been obtained<sup>20</sup> to 2% accuracy by scattering neutrons from atomic electrons. Away from  $Q^2 = 0$ ,  $G_{En}$  is obtained from electron-deuteron elastic and quasi-elastic scattering, but has until now only been measured out to  $Q^2$  of  $1.5 \text{ (GeV/c)}^2$  with errors from 30% to 50%. In that region there are quasi-free measurements<sup>19</sup> dominated by large statistical errors, with  $G_{En}$  extracted from the intercepts of the Rosenbluth plots consistent with  $G_{En} = 0$ , and elastic ed measurements<sup>21</sup> with  $G_{En}$  ranging from zero to about 0.10 with the largest uncertainty from deuteron model dependence.

The electric form factor of the neutron is a particularly important quantity for our understanding of nucleon and nuclear structure. The  $Q^2$  dependence of  $G_{En}$  is related to the charge distribution of the neutral neutron, and is a sensitive test of the symmetry of the ground-state quark wave function.<sup>22</sup> Knowledge of the neutron electric form factor is

essential for accurate calculations of electromagnetic interactions of nuclei, especially the deuteron, which serves as the laboratory for our investigations of the short range nuclear force, meson currents, and relativistic effects.<sup>13</sup> For all these investigations our present knowledge of  $G_{En}$  is highly inadequate. It would even be important to know only if  $G_{En}$  were not strictly zero above  $Q^2 = 0$ . To this end we suggest that measuring the polarization of recoil neutrons following (quasi) elastic scattering of polarized electrons might offer a better possibility to determine  $G_{En}$  than the previous methods.

The neutron is easier to study (at least theoretically) than the deuteron because there are no tensor polarizations, only vector polarizations. Similarly, instead of there being four analyzing powers there is only one, the one called  $A_y$ .

The formula for the full cross section for scattering longitudinally polarized electrons from unpolarized neutrons, including both the first and second scatterings is:

$$\frac{d\sigma}{d\Omega d\Omega_2} = \frac{d\sigma}{d\Omega d\Omega_2} \Big|_0 \left\{ 1 + a p_x A_y \sin\phi_2 \right\} \quad (11)$$

where  $a$  is the electron polarization,  $\frac{d\sigma}{d\Omega d\Omega_2} \Big|_0$  is the double scattering cross section with unpolarized electrons, and  $\phi_2$  is again as indicated in Fig. 1. The only non-zero polarizations are:<sup>23</sup>

$$\begin{aligned} I_0 p_x &= I_0 K_{LS} = -2 \sqrt{\tau(1+\tau)} G_{Mn} G_{En} \tan\left(\frac{1}{2}\theta\right) \\ I_0 p_z &= I_0 K_{LL} = 2\tau \sqrt{(1+\tau) \left(1 + \tau \sin^2\left(\frac{1}{2}\theta\right)\right)} G_{Mn}^2 \sec\left(\frac{1}{2}\theta\right) \tan\left(\frac{1}{2}\theta\right) \\ &= \frac{E + E'}{M} \sqrt{\tau(1+\tau)} G_{Mn}^2 \tan^2\left(\frac{1}{2}\theta\right) \end{aligned} \quad (12)$$

Here

$$I_0 = G_{En}^2 + \tau G_{Mn}^2 [1 + 2(1 + \tau) \tan^2(\frac{1}{2}\theta)],$$

$$\tau = Q^2/4M^2$$
(13)

and  $M$  is the neutron mass. The recoil polarizations  $p_x$  and  $p_z$  are the same as the spin transfer coefficients  $K_{LS}$  and  $K_{LL}$  familiar from nucleon-nucleon scattering,<sup>24</sup> and we have indicated above this alternate notation.

The polarization component  $p_x$  is the most interesting because it is directly proportional to the sought after  $G_{En}$  and it alone appears in the cross section Eq. 11 for double scattering. The component  $p_z$  is less interesting from the point of view of form factors because it is proportional to  $G_{Mn}$ , and it is not directly observable in the second scattering. We will study both components here, however, because under certain experimental conditions, both may be important. The neutron detection system would almost certainly include magnetic fields between the first and second scatterings to sweep away charged particles, and the recoil neutron spins would precess through large angles due to the large neutron magnetic moment. Therefore it would be necessary to know both  $p_x$  and  $p_z$  emerging from the first scattering to calculate the component  $p_x$  entering the second scattering. We shall see below that one might arrange the necessary magnetic fields to actually take advantage of the unavoidable large precession to help reduce the systematic errors.

We have evaluated the formulas for  $p_x$  and  $p_z$  for several choices of neutron form factors and a range of  $Q^2$  and scattering angle  $\theta$ . Figure 5 shows the results as a function of  $\theta$  for fixed  $Q^2$  for one of the Höhler et al. fits.<sup>25</sup> The fact that  $p_x \rightarrow 0$  and  $p_z \rightarrow 1$  at large angles is a general kinematical feature evident from Eqs. 12 and 13. While  $p_x$  grows

with increasing  $\theta$  at small  $\theta$ , the figure of merit (event rate)<sup>1/2</sup> × (polarization) decreases with increasing  $\theta$ . Therefore the choice of  $\theta$  would tend toward forward angles.

In Fig. 6 is plotted the polarization vrs  $Q^2$  at a given electron scattering angle  $\theta = 50^\circ$  for several different form factor models. The results for the fit we<sup>13</sup> called "Best Fit" with  $G_{En}$  from Galster et al.,<sup>21</sup> the Höhler et al.<sup>25</sup> fit 8.2, and the Blatnick and Zovko fit<sup>26</sup> are all quite similar. These correspond to values for  $G_{En}$  consistent with the slope at  $Q^2 = 0$  and rising to approximately 0.05 at  $Q^2 = 1$  (GeV/c)<sup>2</sup> in the middle of the large experimental errors. The IJL fit from Iachello, Jackson, and Lande<sup>27</sup> is determined entirely from a model fit to nucleon form factor data excluding  $G_{En}$  and gives quite different results, with  $G_{En}$  and  $p_x$  passing through zero near  $Q^2 = 1.4$  (GeV/c)<sup>2</sup>. The form "Dipole +  $G_{En} = 0$ " yields  $p_x = 0$  and  $p_z$  indistinguishable from the other phenomenological fits. Finally, the curve labeled "Dipole +  $F_{1n} = 0$ " employs standard dipole forms with the Dirac form factor of the neutron set to zero.<sup>13</sup> This is consistent with a quark model for nucleon structure with the valence quarks in a spatially symmetric ground state, and gives

$$G_{En} = -\tau G_{Mn} = \frac{1.91 \tau}{(1 + 0.71 Q^2)^2} \quad (14)$$

for  $Q^2$  in (GeV/c)<sup>2</sup>. This  $G_{En}$  is at the upper edge of the large experimental error bars on the existing data.

All five models that we used are plausible estimates for  $G_{En}$  spanning the range covered by the present large errors, and these estimates give wide variations in the predictions for  $p_x$ . Since the polarization  $p_z$  is dominated by the better known  $G_{Mn}$ , there is less divergence among the models for this component.

The most likely candidate for the analyzing reaction would be np elastic scattering for which the cross sections are relatively large and the analyzing powers fairly well measured.<sup>4</sup> It seems possible that an analyzer-detector system could be built with an efficiency of  $10^{-4}$  to  $10^{-5}$  with an effective analyzing power of 0.2 to 0.3. To achieve significant count rates with such low detection efficiency would require large beam currents. The signal-to-background ratio would be enhanced by detecting the scattered electrons in coincidence if accidental rates are low. These requirements are nicely matched to the projected capabilities of the next generation of high-duty-factor, high-current electron accelerator in the several-GeV region.

Since the neutron target (probably deuterium) would also inevitably contain protons, a sweeping field between the first and second scattering would be necessary to remove background. With a vertical sweeping field charged particles are swept sideways in the lab and do not introduce a possible spurious asymmetry in the analyzer measuring the up-down asymmetry from the  $p_x$  component. The neutron spin then precesses around the vertical direction as shown in Fig. 7. This precession rotates the large initial  $p_z$  component into the x direction at the second scattering, thus increasing the up-down asymmetry in the analyzer. Horizontal sweeping fields would not be optimum because  $p_z$  would precess into the y direction introducing an unwanted left-right asymmetry, and the charged particle background would be highly asymmetric in the up-down direction.

To indicate the possible sensitivity of such a measurement to the predicted  $G_{En}$  and  $G_{Mn}$ , we show in Fig. 8 for a scattering angle  $\theta = 50^\circ$  the variation of the component  $p_x$  vrs precession angle  $\omega$ , as in Fig. 7, for the neutron models described in Fig. 6. In principle, data with

sufficient accuracy and range of precession angle  $\omega$  could be used to separate  $G_{En}$  and  $G_{Mn}$  from the phase and amplitude of the curve as in Fig. 8. If the precision or range were too limited, it may still be possible to extract  $G_{En}$  from the intercept at  $\vec{H} = 0$ . One could either calculate the effect of the sweeping field assuming knowledge of  $G_{Mn}$ , determined more precisely from the angular distribution, to extract the desired initial  $p_x$ , or alternatively, one could measure large up-down asymmetries with  $\pm \vec{H}$  sweeping fields and determine  $p_x$  at  $\vec{H} = 0$  by extrapolation. While this technique would not directly increase the sensitivity to  $G_{En}$ , because the increased asymmetry is due to  $G_{Mn}$ , it would be advantageous for establishing confidence in the method by increasing the size of the asymmetry signal in a controlled way, and for reducing the systematic errors by averaging over symmetric measurements. From Fig. 8 we see that for analyzing power of 0.2 to 0.3 an experiment with the capacity to measure  $10^3$  to  $10^4$  counts could distinguish between some of the models for  $G_{En}$ , assuming that systematic errors are not dominating.

While such double scattering experiments with neutrons would be difficult, we think they merit serious consideration because of several advantages they offer. First, the desired small quantity  $G_{En}$  is directly proportional to the up-down asymmetry signal (extrapolated to  $\vec{H} = 0$ ), and is not buried in strong competition with the larger  $G_{Mn}$ , as in the Rosenbluth method, or available only after a model dependent analysis, as in elastic ed scattering. Also the quantity of interest is extracted directly from a ratio measurement (up-down/up+down) which provides the additional advantage that the result does not depend on any knowledge of absolute normalizations of the beam-target-analyzer system. All that is

required is adequate counting rates and knowledge of the effective analyzing power  $A_y$  to extract  $p_x$ . Finally, measurements with opposite electron polarization and with unpolarized electron beams can be used to eliminate spurious asymmetries. The compelling physics interest in  $G_{En}$  should provide strong motivation to attempt even a difficult experiment.

#### D. The Proton

The value of  $G_{Ep}$  is much better known than  $G_{En}$  -- particularly at very low  $Q^2$  where it dominates elastic scattering from free protons.<sup>28</sup> However, for  $Q^2 \gtrsim 1(\text{GeV}/c)^2$ ,  $G_{Mp}$  dominates the cross section, and our knowledge of  $G_{Ep}$  fades out at  $Q^2 \simeq 3(\text{GeV}/c)^2$ , where the current<sup>29</sup> experimental uncertainty is of the order of 100%. Better measurements of  $G_{Ep}$  in the  $Q^2$  region between 2 and 4  $(\text{GeV}/c)^2$  would be of great value to both nuclear and particle physics.

In Fig. 9 are plotted the vector polarizations  $p_x$  and  $p_z$  of the recoiling proton for various  $Q^2$  versus electron scattering angle for the Höhler et al. model fit 8.2. There we see the same kinematical feature as for the neutron that  $p_x \rightarrow 0$  and  $p_z \rightarrow 1$  for large angles.

In Fig. 10,  $p_z$  and  $p_x$  are given as a function of  $Q^2$  for a fixed angle of  $40^\circ$  and five different models: the dipole form (which, on the graph, cannot be distinguished from the model of Blatnik and Zovko<sup>26</sup>), the IJL model of Ref. 27, and two models of Höhler et al.<sup>25</sup> Note that the models differ significantly in the region of  $Q^2 = 2$  to 4  $(\text{GeV}/c)^2$ , and that the polarizations are large.

The analyzing powers for protons are also somewhat larger than for neutrons<sup>4</sup> varying between 0.4 and 0.3 in the region of  $Q^2 \lesssim 4(\text{GeV}/c)^2$ . For higher  $Q^2$  (i.e., higher energy protons) the analyzing powers and ep

cross sections begin to fall off, so that the experiment proposed here becomes increasingly difficult. Also, if the recoil proton detector-analyzer employs magnetic fields, then, as for the neutron, there will be large precession due to the large  $g-2$  factor. Determination of the recoil  $p_x$  and  $p_z$  by variation of the precession angle would be somewhat more complicated in this case, however, because the precession is correlated with the bend angle, which for a given geometry and field, is fixed by the recoil proton momentum or  $Q^2$ .

A 10% measurement of  $p_x$  at a  $Q^2$  of 4 (GeV/c)<sup>2</sup> would just be sufficient to distinguish the IJL, Dipole, and Höhler models from each other. Since the analyzing power at the appropriate momentum (about 3 GeV/c) is known to about the same accuracy, better measurements of the analyzing power would be helpful but are not essential. The expected asymmetry at  $Q^2 = 2(\text{GeV}/c)^2$  for a 100% polarized electron beam would be about 10%, and a 10% measurement of this asymmetry requires about  $10^4$  counts.

## II. THEORETICAL CALCULATIONS

We shall describe the polarization calculations for spin-1 particles. The calculation of cross sections from current matrix elements is standard and will merit only a few remarks at the beginning, and the remainder of the section will be devoted to defining and calculating the polarizations and analyzing powers.

The momentum and helicity of the incoming and outgoing electron are  $(k, \tau)$  and  $(k', \tau')$  respectively, and the corresponding quantities for the deuteron are  $(D, \lambda)$  and  $(D', \lambda')$ . The matrix element is

$$\mathcal{M} = ie^2 \bar{u}(k', \tau') \gamma^\mu u(k, \tau) \frac{1}{q} \langle D' \lambda' | j_\mu | D \lambda \rangle \quad (15)$$

The electromagnetic current for the deuteron is

$$\begin{aligned} \langle D'\lambda' | j_\mu | D\lambda \rangle = & - \left\{ \left[ G_1 \xi'^* \cdot \xi - G_3 \frac{(\xi'^* \cdot q)(\xi \cdot q)}{2M_d^2} \right] (D + D')_\mu \right. \\ & \left. + G_2 \left[ \xi_\mu (\xi'^* \cdot q) - \xi_\mu'^* (\xi \cdot q) \right] \right\}, \end{aligned} \quad (16)$$

where

$$\begin{aligned} G_M &= G_2 \\ G_Q &= G_1 - G_2 + (1 + \eta) G_3 \\ G_C &= G_1 + \frac{2}{3} \eta G_Q \end{aligned} \quad (17)$$

and  $\xi = \xi(\lambda)$  and  $\xi' = \xi'(\lambda')$  are the polarization four-vectors of the initial and final deuteron and satisfy  $\xi \cdot D = \xi' \cdot D' = 0$ . If the initial electron is longitudinally polarized, then the cross section will be proportional to (for  $m_e = 0$ )

$$\begin{aligned} L^{\mu\nu} &= \sum_{\tau'} \bar{u}(k'\tau') \gamma^\mu u(k\tau) \bar{u}(k\tau) \gamma^\nu u(k'\tau') \\ &= \frac{1}{2} \text{Tr } \not{k}' \gamma^\mu (1 + a\gamma_5) \not{k} \gamma^\nu \\ &= 2 \left[ k'^\mu k^\nu + k^\mu k'^\nu - k \cdot k' q^{\mu\nu} + ia \varepsilon^{\mu\nu\sigma\tau} k_\sigma k'_\tau \right] \end{aligned} \quad (18)$$

where  $a$  is the electron's polarization ( $a = \pm 1$  for the pure helicity state implied by the first line above, and  $|a| \leq 1$  if one does the weighted sum appropriate for a partially polarized beam).

When we calculate the cross section for producing final state deuterons in some definite polarization state

$$\xi = \sum_{\lambda=-1}^1 b_\lambda \xi'(\lambda) \quad (19)$$

we get

$$\frac{d\sigma_{\xi}}{d\Omega} = \sum_{\lambda\lambda'} b_{\lambda}^* b_{\lambda'} \frac{d\sigma_{\lambda\lambda'}}{d\Omega} \quad (20)$$

where

$$\frac{d\sigma_{\lambda\lambda'}}{d\Omega} = \frac{d\sigma}{d\Omega} \Big|_{NS} \left( A + B \tan^2 \left( \frac{1}{2} \theta \right) \right) \times \frac{1}{3} \xi_{\alpha}^{\prime*}(\lambda) \rho^{\alpha\beta} \xi_{\beta}'(\lambda') . \quad (21)$$

Here  $\rho^{\alpha\beta}$  is a relativistic version of the density matrix and completely describes the polarization of the outgoing deuteron. Note that both  $\xi'(\lambda')$  and  $\xi'^*(\lambda)$  refer to the outgoing deuteron. The normalization of  $\rho$  is

$$\sum_{\lambda' = -1}^1 \frac{1}{3} \xi_{\alpha}^{\prime*}(\lambda') \rho^{\alpha\beta} \xi_{\beta}'(\lambda') = 1 , \quad (22)$$

which leads to the correct cross section for the case when the final polarization is not measured.

The vector and tensor polarizations are defined from the density matrix. Note that  $\xi_{\alpha}^{\prime*} \rho^{\alpha\beta} \xi_{\beta}'$  is a covariant object, so that we may study it in a reference frame of our choosing. In the rest frame of the deuteron, the polarization vectors have only spatial components, and  $\rho$  can be treated as a  $3 \times 3$  matrix. We then use the standard non-relativistic conventions as recorded below to define the vector and tensor polarizations. If one wishes, the  $3 \times 3$  matrices below can be thought of as the space parts of  $4 \times 4$  matrices with the unwritten components being zero, and their form in an arbitrary frame can be obtained by boosting. We choose our coordinate axes as shown in Fig. 1, and write  $\rho$  in terms of Cartesian tensors,<sup>8</sup>

$$\rho = I + \frac{3}{2} (p_x \mathcal{P}_x + p_y \mathcal{P}_y + p_z \mathcal{P}_z) + \frac{1}{2} p_{zz} \mathcal{P}_{zz} + \frac{2}{3} p_{xz} \mathcal{P}_{xz} + \frac{1}{6} (p_{xx} - p_{yy}) (\mathcal{P}_{xx} - \mathcal{P}_{yy}) \quad (23)$$

$$\mathcal{P}_x = S_x = \begin{pmatrix} 0 & 0 & 0 \\ 0 & 0 & -i \\ 0 & i & 0 \end{pmatrix}; \quad \mathcal{P}_y = S_y = \begin{pmatrix} 0 & 0 & i \\ 0 & 0 & 0 \\ -i & 0 & 0 \end{pmatrix}; \quad \mathcal{P}_z = S_z = \begin{pmatrix} 0 & -i & 0 \\ i & 0 & 0 \\ 0 & 0 & 0 \end{pmatrix};$$

$$\mathcal{P}_{zz} = 3\mathcal{P}_z^2 - 2 = \begin{pmatrix} 1 & 0 & 0 \\ 0 & 1 & 0 \\ 0 & 0 & -2 \end{pmatrix}; \quad \mathcal{P}_{xx} - \mathcal{P}_{yy} = \begin{pmatrix} -3 & 0 & 0 \\ 0 & 3 & 0 \\ 0 & 0 & 0 \end{pmatrix};$$

$$\mathcal{P}_{xz} = \frac{3}{2} (\mathcal{P}_x \mathcal{P}_z + \mathcal{P}_z \mathcal{P}_x) = \frac{3}{2} \begin{pmatrix} 0 & 0 & -1 \\ 0 & 0 & 0 \\ 1 & 0 & 0 \end{pmatrix}. \quad (24)$$

For example, consider calculating the cross section for producing a final state polarization in the  $\pm x$  direction. This means that the polarizations are eigenstates of  $S_x$  with eigenvalues  $\pm 1$ ,

$$S_x \xi_{\pm x} = \pm \xi_{\pm x}, \quad (25)$$

so

$$\xi_{\pm x} = \frac{1}{\sqrt{2}} (0, \mp 1, -i) \quad (26)$$

in the rest frame of the final deuteron or

$$i\xi_{\pm x} = -\frac{1}{\sqrt{2}} \xi'(0) \pm \frac{1}{2} (\xi'(+1) + \xi'(-1)) \quad (27)$$

in general. We then get

$$\frac{d\sigma_{+x}}{d\Omega} - \frac{d\sigma_{-x}}{d\Omega} = \frac{d\sigma}{d\Omega} \Big|_{NS} I_0 P_x. \quad (28)$$

The quantity on the left is straightforward to calculate, and leads to the expression for  $p_x$  quoted earlier. Similar exercises yield the other vector and tensor polarizations.

Incidentally, the symmetric and antisymmetric parts of  $L_{\mu\nu}$  induce terms of corresponding symmetry in the density matrix. The facts that the tensor polarization matrices are symmetric and that the part of  $L_{\mu\nu}$  that depends on the electron polarization is antisymmetric leads to the statement made earlier that the tensor polarizations are not changed by the electron polarization.

To measure the polarizations  $p_i$  and  $p_{ij}$  we must do a second scattering from another target which is called the analyzer. The dependence of the cross section upon the polarization of the entering deuteron can be studied with a formalism like the density matrix given above. If the entering deuteron is in a pure polarization state  $\xi$ , then

$$\frac{d\sigma}{d\Omega_2} = \sum_{\lambda\lambda'} b_{\lambda'}^* b_{\lambda} \frac{d\sigma_{\lambda'\lambda}}{d\Omega} \quad (29)$$

where

$$\frac{d\sigma_{\lambda'\lambda}}{d\Omega} = I_2 \xi_{\alpha}^*(\lambda') \sum^{\alpha\beta} \xi_{\beta}(\lambda) \quad (30)$$

In the rest frame of the entering deuteron,  $\Sigma$  may be treated as a  $3 \times 3$  matrix, with,

$$\begin{aligned} \Sigma = & 1 + \frac{3}{2} A_y \mathcal{P}_{y'} + \frac{1}{2} A_{zz} \mathcal{P}_{z'z'} + \frac{2}{3} A_{xz} \mathcal{P}_{x'z'} \\ & + \frac{1}{6} (A_{xx} - A_{yy}) (\mathcal{P}_{x'x'} - \mathcal{P}_{y'y'}) \end{aligned} \quad (31)$$

Components of  $A$  not listed above are zero by parity invariance.

The primes remind us that the two scatterings are not in the same plane. The unprimed coordinates axes are shown in Fig. 1; the z-axis is

along the direction of the deuteron exiting the ed scattering and the x-axis is in the ed scattering plane. The primed coordinates are for the second scattering, so the z' and z-axis are the same, but the x'-axis is in the plane of the analyzing scattering. The primed axes are related to the unprimed axes by a rotation about the z-axis<sup>8</sup> through angle  $\phi_2$ . Thus, if  $(\mathcal{P}_{y'})_{i'j'}$  and  $(\mathcal{P}_y)_{ij}$  are the components of  $\mathcal{P}_y$ , in the primed and unprimed coordinates, respectively, we have

$$(\mathcal{P}_{y'})_{ij} = R_{ii'} R_{jj'} (\mathcal{P}_{y'})_{i'j'} \quad (32)$$

with

$$R = \begin{pmatrix} \cos\phi_2 & -\sin\phi_2 & 0 \\ \sin\phi_2 & \cos\phi_2 & 0 \\ 0 & 0 & 1 \end{pmatrix} \quad (33)$$

$\mathcal{P}_{y'}$ , in the primed coordinates has the same form as  $\mathcal{P}_y$  in the unprimed coordinates, so that

$$\mathcal{P}_{y'} = \mathcal{P}_y \cos\phi_2 + \mathcal{P}_x \sin\phi_2 \quad (34)$$

The other  $3 \times 3$  matrices can be rotated similarly.

Of course, the entering deuteron is in a linear combination of polarization states given by its density matrix. The overall cross section is obtained from

$$\frac{d\sigma}{d\Omega d\Omega_2} = \frac{d\sigma}{d\Omega d\Omega_2} \Big|_0 \times \text{Tr} \left( \frac{1}{3} \rho \Sigma \right) \quad (35)$$

which yields the result given in Eq. 4.

#### Acknowledgements

This research was supported principally by the National Science Foundation (Grants PHY78-09378 and PHY79-19071) and in addition by the Department of Energy (Contract No. DE-AC03-76SF00515).

REFERENCES

1. M. J. Alguard, et al., NIM 163, 29 (1979), Phys. Rev. Lett. 37, 1258 (1976).
2. C. K. Sinclair et al., in AIP Conference Proceedings No. 35, Particles and Fields Subseries No. 12; High Energy Physics with Polarized Beams and Targets, Argonne, 1976, Ed. M. L. Marshak (American Institute of Phys., New York, 1976), p. 424; and C. Prescott et al., Phys. Lett. 77B, 347 (1978).
3. C. K. Sinclair, SLAC, private communication.
4. See, for example, R. Diebold, et al., Phys. Rev. Lett. 35, 632 (1975), and references therein.
5. J. Button and R. Mermod, Phys. Rev. 118, 1333 (1960).
6. J. Baldwin et al., Phys. Rev. 103, 1502 (1956).
7. Transversely polarized electrons give effects of order  $m_e/E$ , where E is the incident electron lab energy. All our formulas are given with  $m_e = 0$  and in the one photon exchange approximation.
8. G. G. Ohlsen, Rep. Prog. Phys. 35, 717 (1972); G. G. Ohlsen and P. W. Keaton, Jr., Nucl. Instrum. Methods 109, 41 (1973); G. C. Salzman, C. K. Mitchell and G. G. Ohlsen, ibid, 61 (1973).
9. D. Schildknecht, Phys. Lett. 10, 254 (1964); M. Gourdin and C. A. Piketty, Nuovo Cimento 32, 1137 (1964).
10. J. S. Levinger, Acta Phys. Hungaria 33, 135 (1973); T. Brady, E. Tomusiak, and J. S. Levinger, Can. J. Physics 52, 1322 (1974).
11. M. J. Moravcsik and J. Ghosh, Phys. Rev. Lett. 32, 321 (1974).
12. M. I. Haftel, L. Mathelitsch, and H.F.K. Zingl, Graz preprint UNIGRAZ-UTP 10/79.

13. R. G. Arnold, C. E. Carlson, and F. Gross, Phys. Rev. C21, 1426 (1980).
14. D. O. Riska and G. E. Brown, Phys. Lett. 38B, 193 (1972).
15. K. Holinde and R. Machleidt, Nucl. Phys. A247, 479 (1976), and private communication.
16. R. Reid, Ann. Phys. (N.Y.) 50, 411 (1968).
17. E. Lomon and H. Feshbach, Ann. Phys. (N.Y.) 48, 94 (1968).
18. W. W. Buck and F. Gross, Phys. Rev. D20, 2361 (1979).
19. W. Bartel et al., Nucl. Phys. B58, 429 (1973); K. Hansen et al., Phys. Rev. D8, 753 (1973).
20. V. E. Krohn and G. R. Ringo, Phys. Rev. 148, 1303 (1966); D8, 1305 (1973)
21. S. Galster et al., Nucl. Phys. B32, 221 (1971).
22. See, for example, R. T. Van de Walle, Subnuclear Physics Series, Ed. A. Zichichi, Vol. 17, "Pointlike Structure Inside and Outside Hadrons," Erice, Sicily (1979), to be published; and references therein.
23. N. Dombey, Rev. Mod. Phys. 41, 236 (1969); J. Scofield, Phys. Rev. 113, 1599 (1959) and 141, 1352 (1966); A. I. Akhiezer and M. P. Rekalov, Fiz. Chast. Atom. Yad. 4, 662 (1973) [translation: Sov. J. Particles Nucl. 4, 277 (1974)].
24. F. Halzen and G. Thomas, Phys. Rev. D10, 344 (1974), and A. Yokosawa, in AIP Conference Proceedings No. 41, Nucleon-Nucleon Interactions - 1977, Vancouver, Ed. H. Fearing et al. (American Institute of Physics, New York 1978), p. 59.
25. G. Höhler et al., Nuc. Phys. B114, 505 (1976).
26. S. Blatnik and N. Zovko, Acta Physica Austriaca, 39, 62 (1974).

27. F. Iachello, A. Johnson, and A. Lande, Phys. Lett 43 B, 191 (1973).
28. F. Borkowski, et al., Nucl. Phys. B93, 461 (1975).
29. J. Litt, et al., Phys. Lett. 31B, 40 (1970).

FIGURE CAPTIONS

1. Definition of electron scattering, recoil particle, and second scattering coordinate systems. The recoil coordinates  $xz$  are in the electron scattering plane.
2. Recoil deuteron polarization components a)  $p_x$ , b)  $p_z$ , c)  $p_{xz}$ , d)  $p_{zz}$ , and e)  $(p_{xx} - p_{yy})$  at selected values of  $Q^2$  versus electron scattering angle  $\theta$  for one choice of deuteron model, HM3 (Ref. 15). These results were calculated relativistically using the formulas of Ref. 13 and the nucleon form factors we call Best Fit. The electron polarization is 1.0. Note, the vertical scale for component  $p_{zz}$  is a factor of five larger than that for the other components.
3. Recoil deuteron polarization components a)  $p_x$ , b)  $p_z$ , c)  $p_{xz}$ , d)  $p_{zz}$ , and e)  $(p_{xx} - p_{yy})$  at electron scattering angle  $\theta = 40^\circ$  versus  $Q^2$  for various deuteron models. The curve labeled RSC-NR is the Reid soft core model (Ref. 16) calculated nonrelativistically. The curves labeled Relativistic were calculated using the relativistic formulas of Ref. 13 and the following deuteron models: RSC -- Reid soft core; HM3 -- one of the Holinde-Machleidt Bonn potentials (Ref. 15); LF-4.5% -- Loman-Feshbach boundary condition model with 4.5% D state (Ref. 17);  $\lambda = 0.4$  -- a 4-component relativistic model (Ref. 18). The electron polarization is 1.0. Note, the vertical scale for components  $p_{xz}$  and  $p_{zz}$  is a factor of ten larger than that for the other components.

4. Ratio of recoil deuteron polarization components  $p_x$  and  $p_{xz}$  at electron scattering angle  $\theta = 40^\circ$  versus  $Q^2$  for the same deuteron models as in Fig. 3.
5. Recoil neutron polarization components a)  $p_z$  and b)  $p_x$  at selected  $Q^2$  versus electron scattering angle  $\theta$  for one choice of nucleon form factors, fit 8.2 from Höhler et al. (Ref. 25).
6. Recoil neutron polarization components a)  $p_z$  and b)  $p_x$  at electron scattering angle  $\theta = 50^\circ$  for various nucleon form factors. The solid curve is for  $G_{Mn}$  of dipole form with  $G_{En}$  set to zero, which yields  $p_x = 0$ . The results for the two fits labeled Best Fit (Ref. 13) and Höhler 8.2 are indistinguishable. The dotted curve labeled BZ is from Blatnick and Zovko (Ref. 26), and IJL is from Ref. 27. The curve labeled Dipole +  $F_{1n} = 0$  was first suggested in Ref. 13 as an example for  $G_{En}$  consistent with the present data for  $A(Q^2)$  and the quark model for nucleon structure with valence quarks in a spatially symmetric ground state.
7. Definition of the precession angle  $\omega$  for neutrons with polarization components  $p_x$  and  $p_z$  recoiling along the z direction through a magnetic field  $\vec{H}$  oriented along the y axis.
8. Recoil neutron transverse polarization  $p_x$  at  $Q^2 = 1.0 \text{ (GeV/c)}^2$  and  $\theta = 50^\circ$  versus precession angle  $\omega$  as defined in Fig. 7. The various nucleon form factors used are the same as in Fig. 6.

9. Recoil proton polarization components a)  $p_z$  and b)  $p_x$  at selected values of  $Q^2$  versus electron scattering angle  $\theta$  for one choice of nucleon form factor, fit 8.2 from Höhler et al. (Ref. 25).
  
10. Recoil proton polarization components a)  $p_z$  and b)  $p_x$  at electron scattering angle  $\theta = 40^\circ$  for various nucleon form factors. The results for Dipole and the fit BZ of Blatnick and Zovko (Ref. 26) are indistinguishable. The Höhler et al. fit 8.2 (Ref. 25) is a fit to both neutron and proton data, while their fit 5.3 is a fit to proton data only. The IJL curve is from Ref. 27.

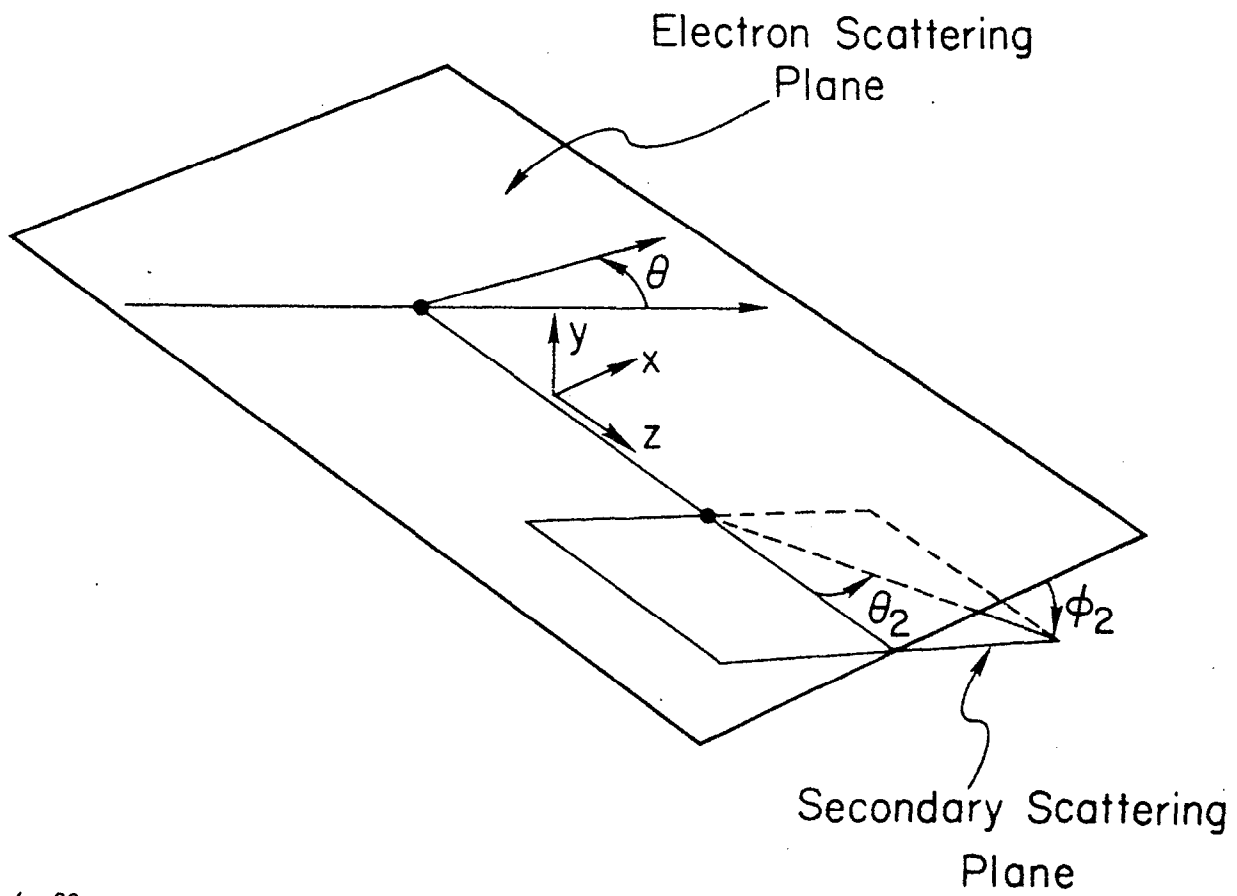


Fig. 1

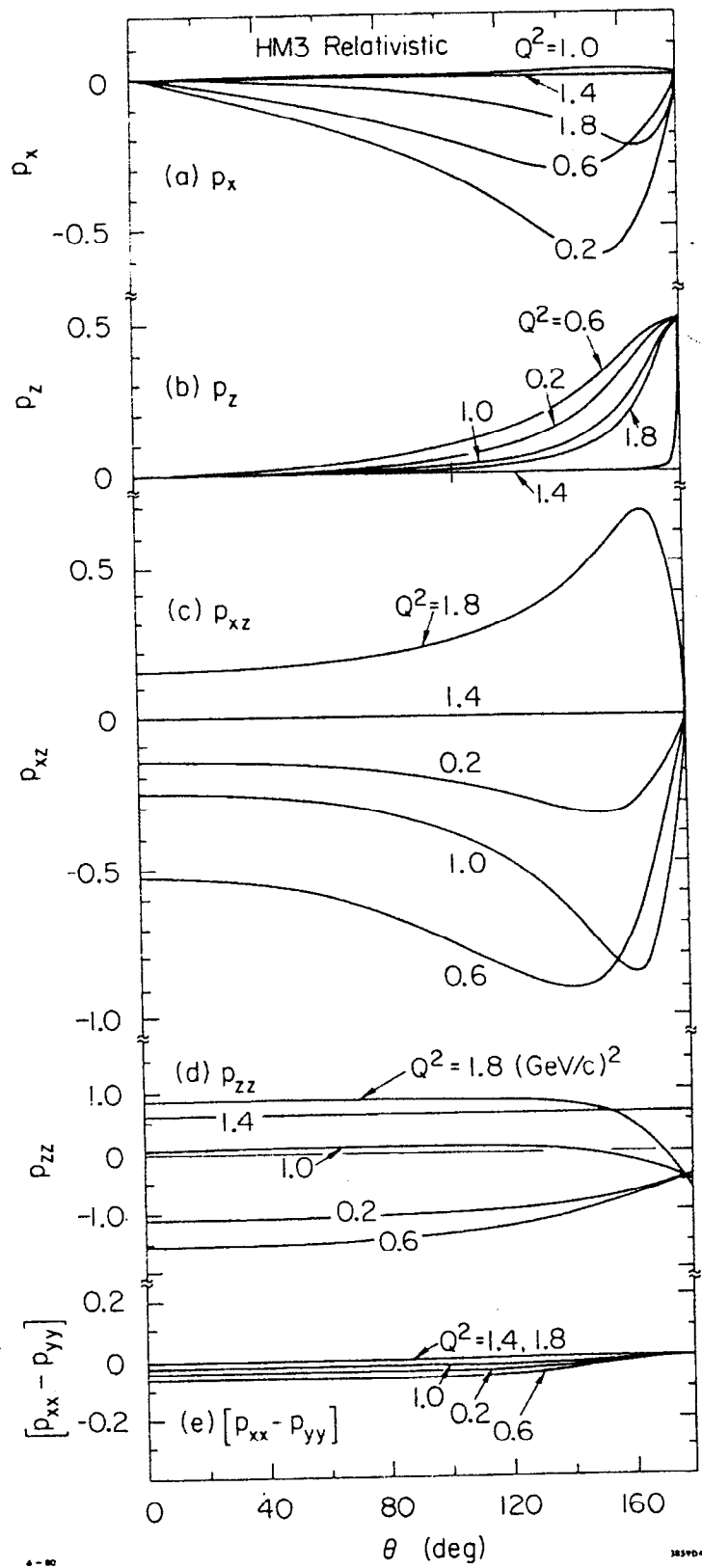


Fig. 2

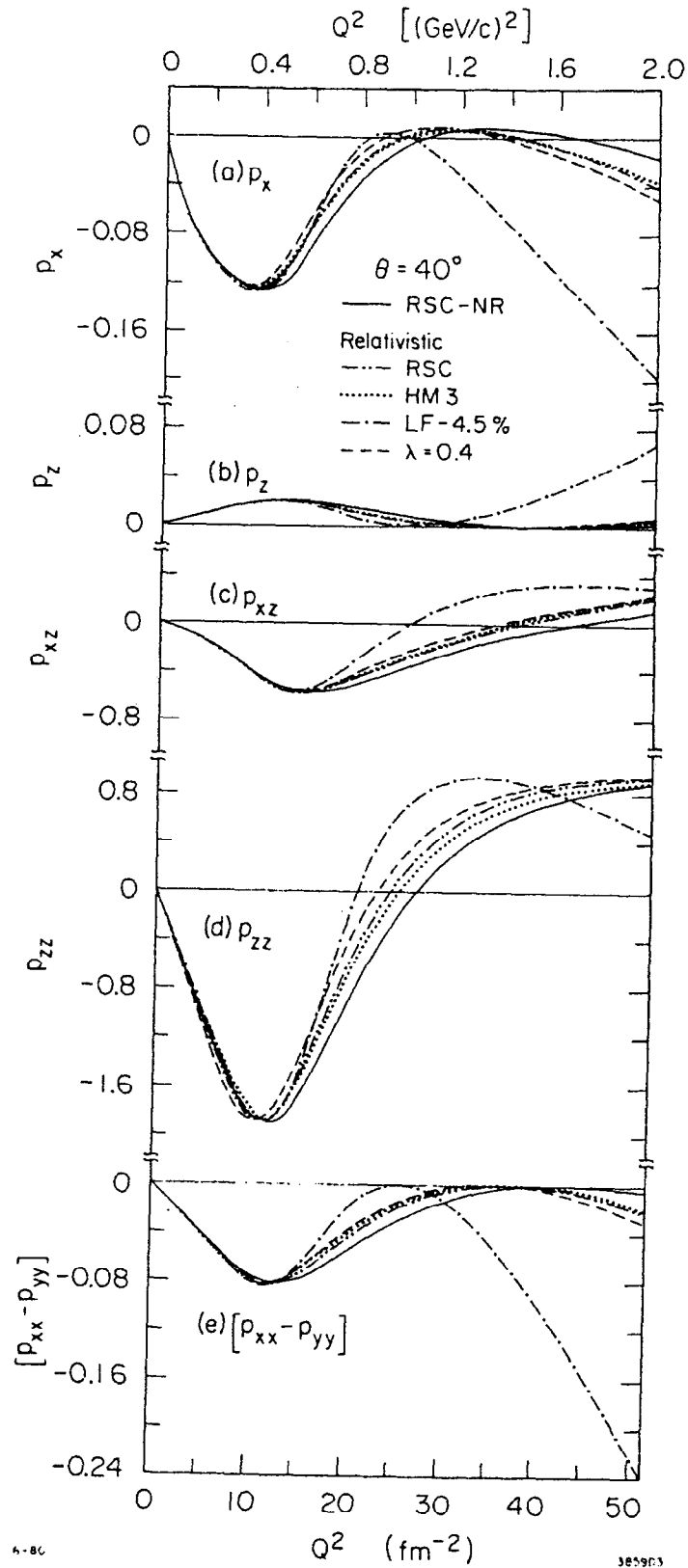


Fig. 3

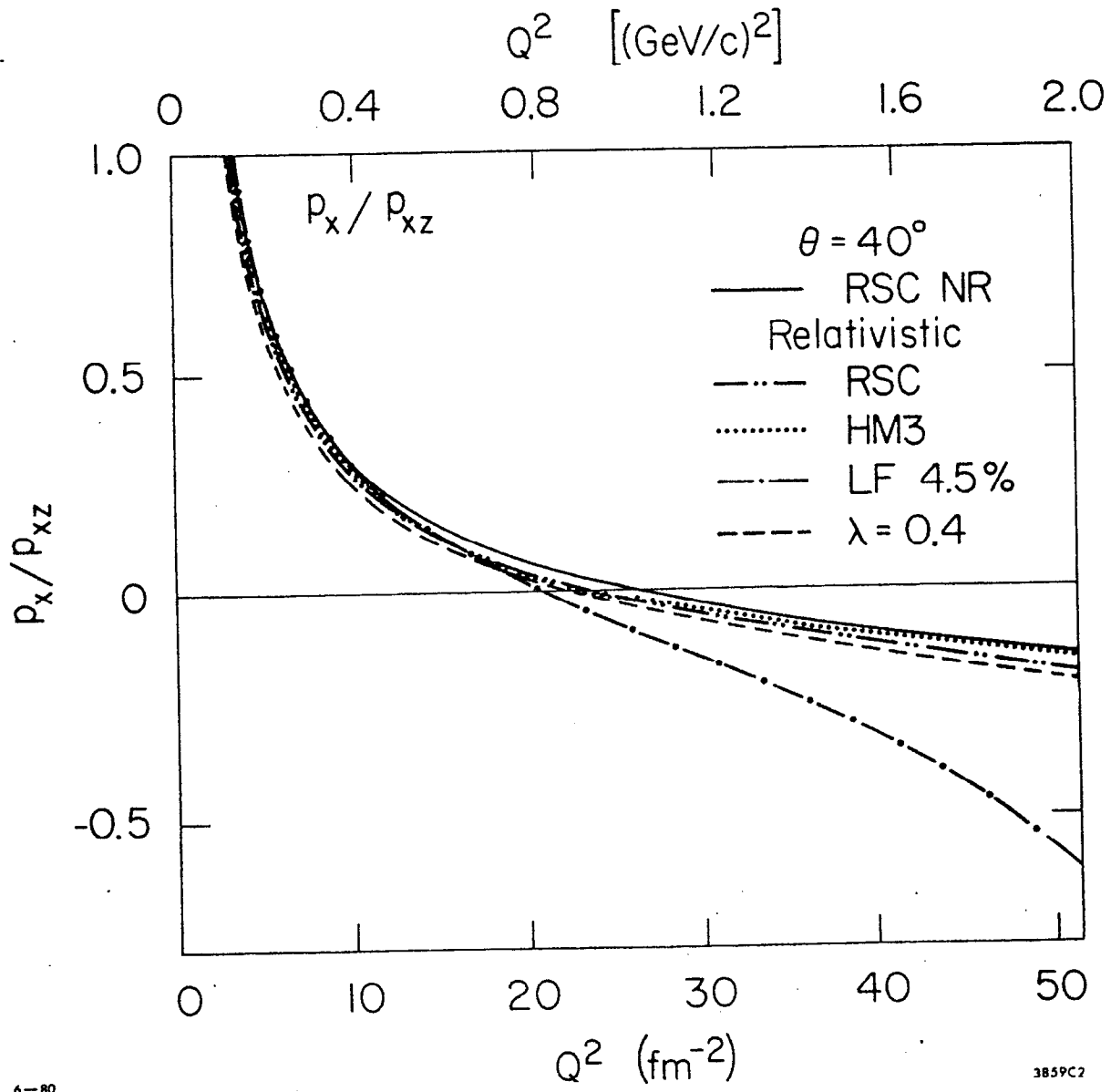


Fig. 4

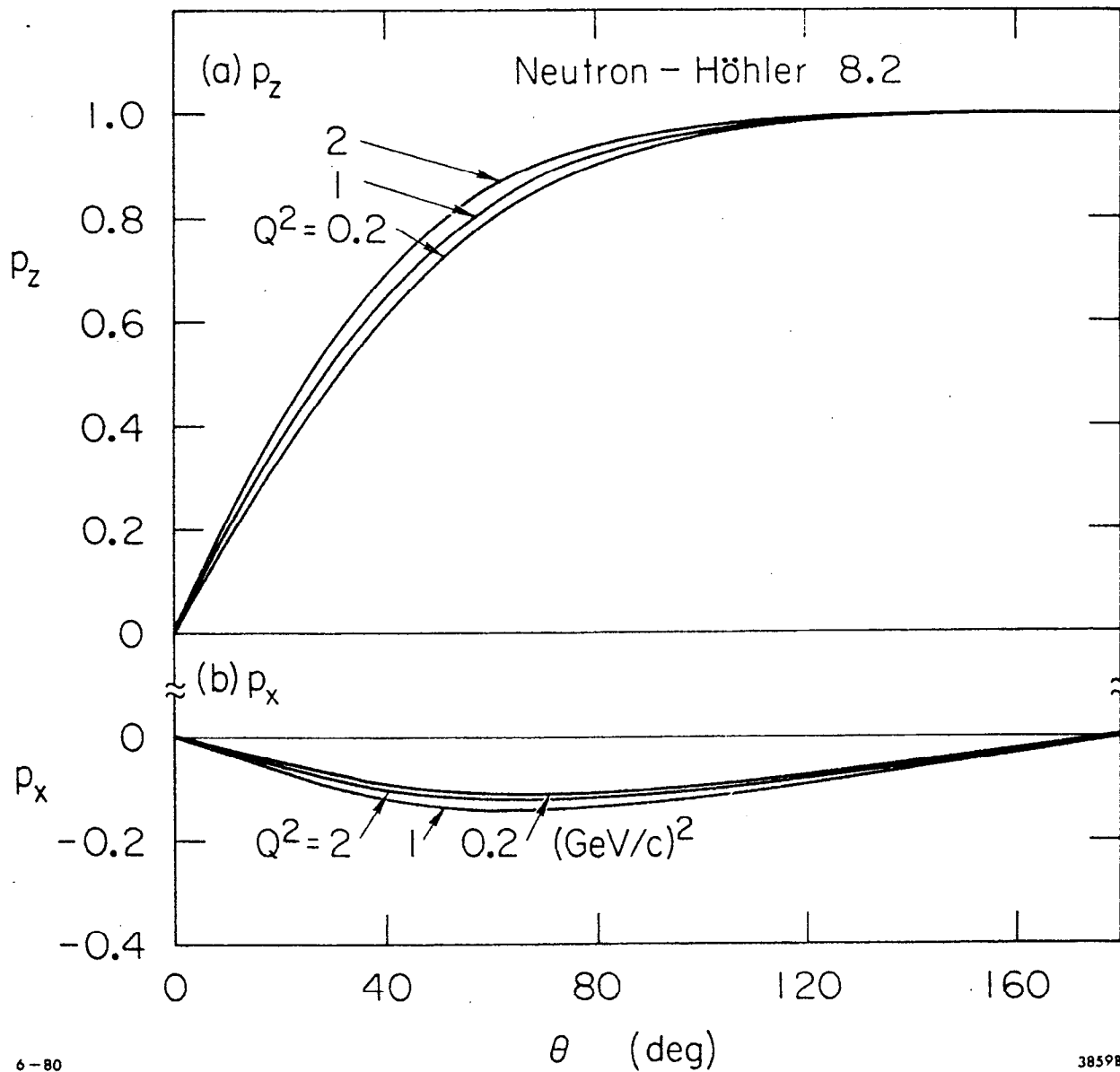


Fig. 5

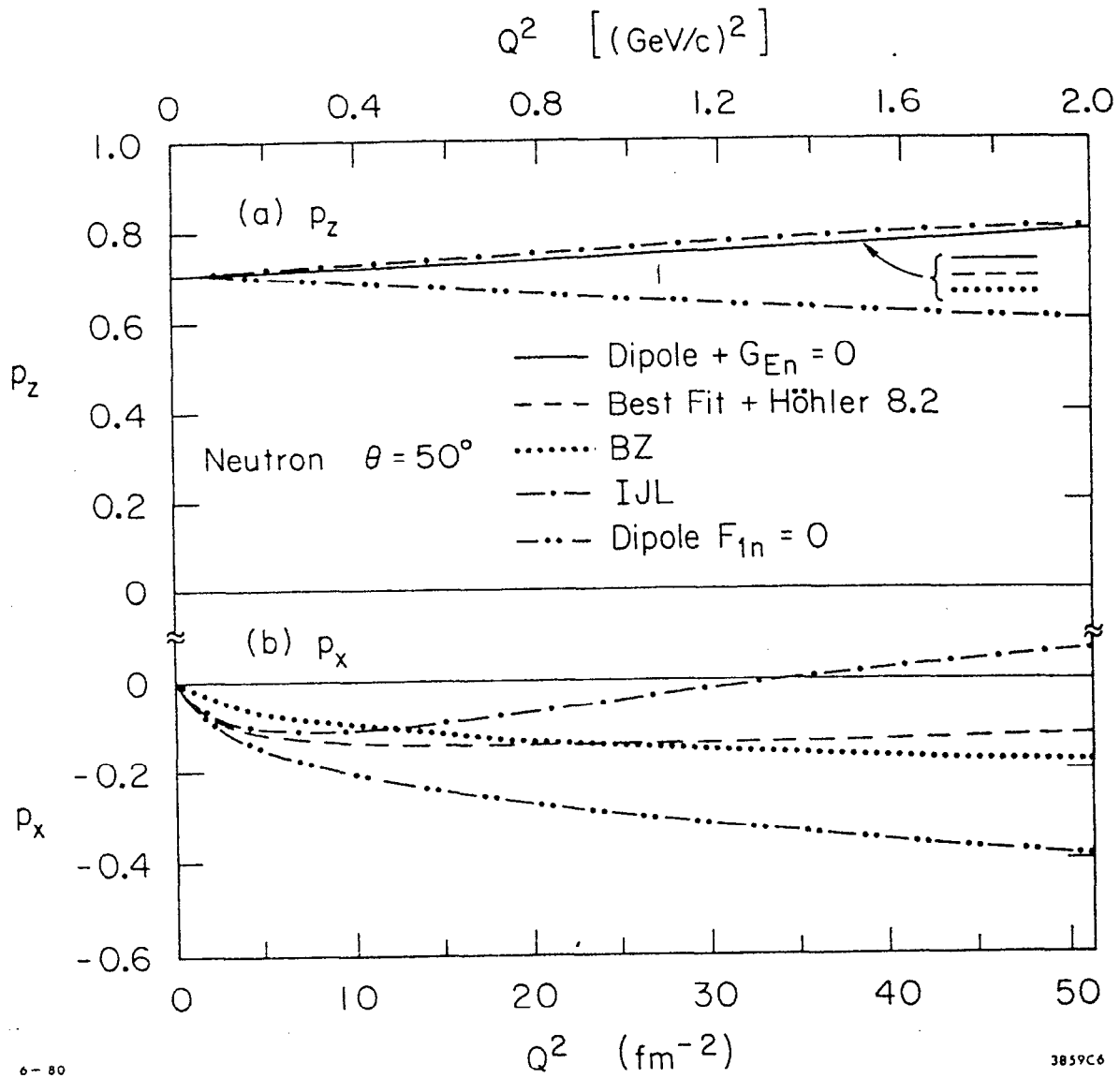
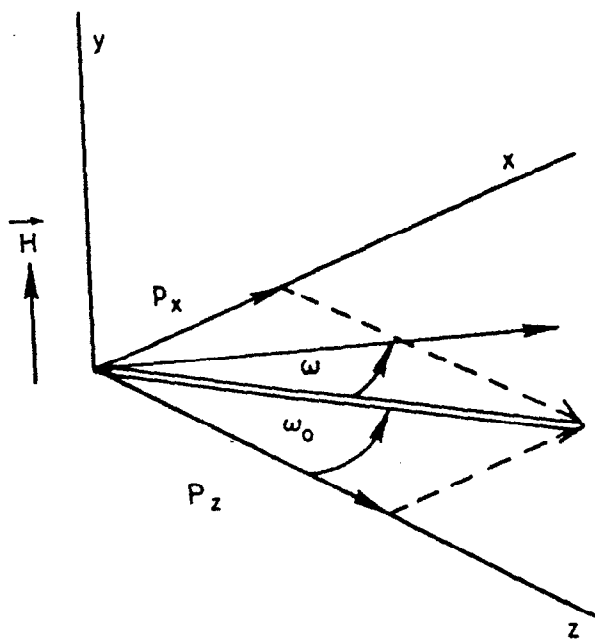


Fig. 6



6-80

3859A7

Fig. 7

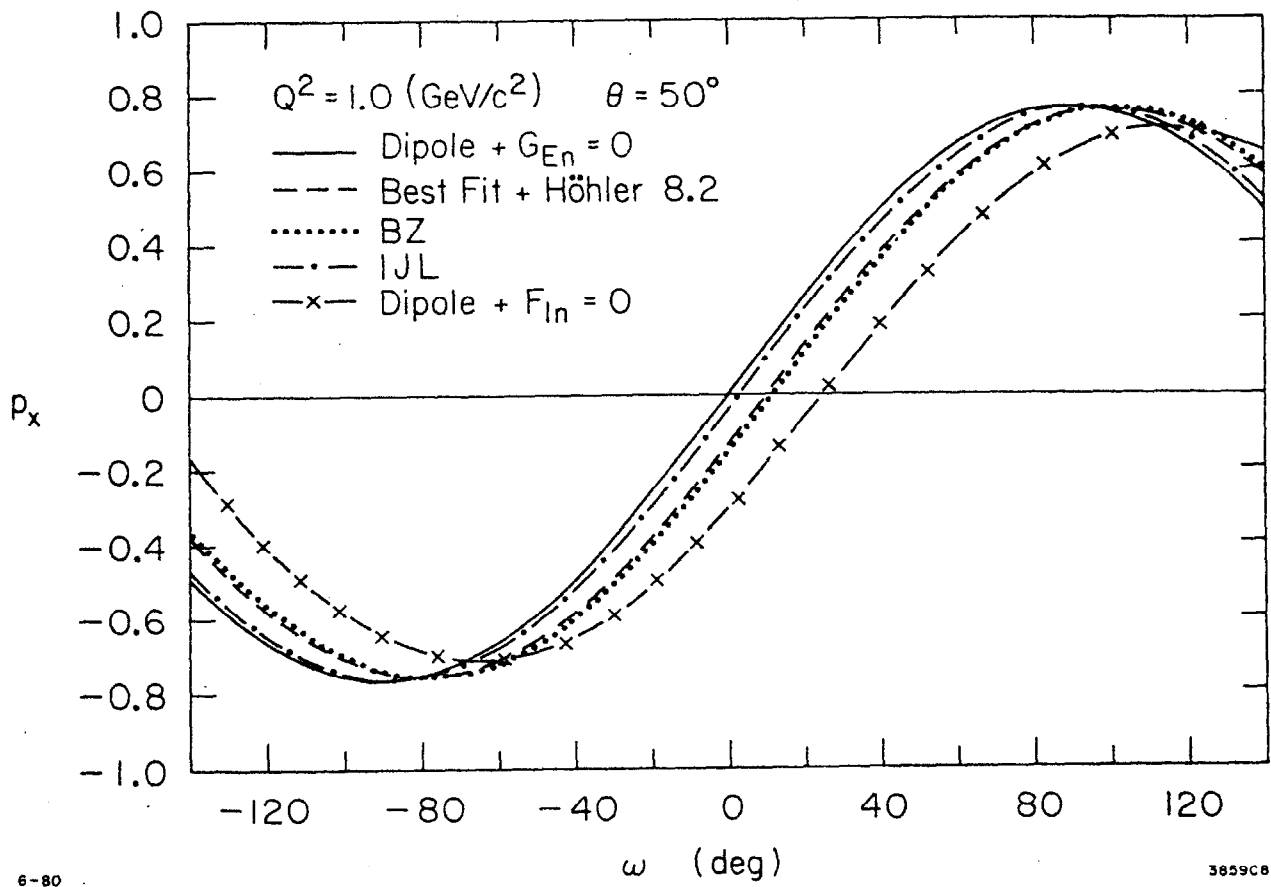


Fig. 8

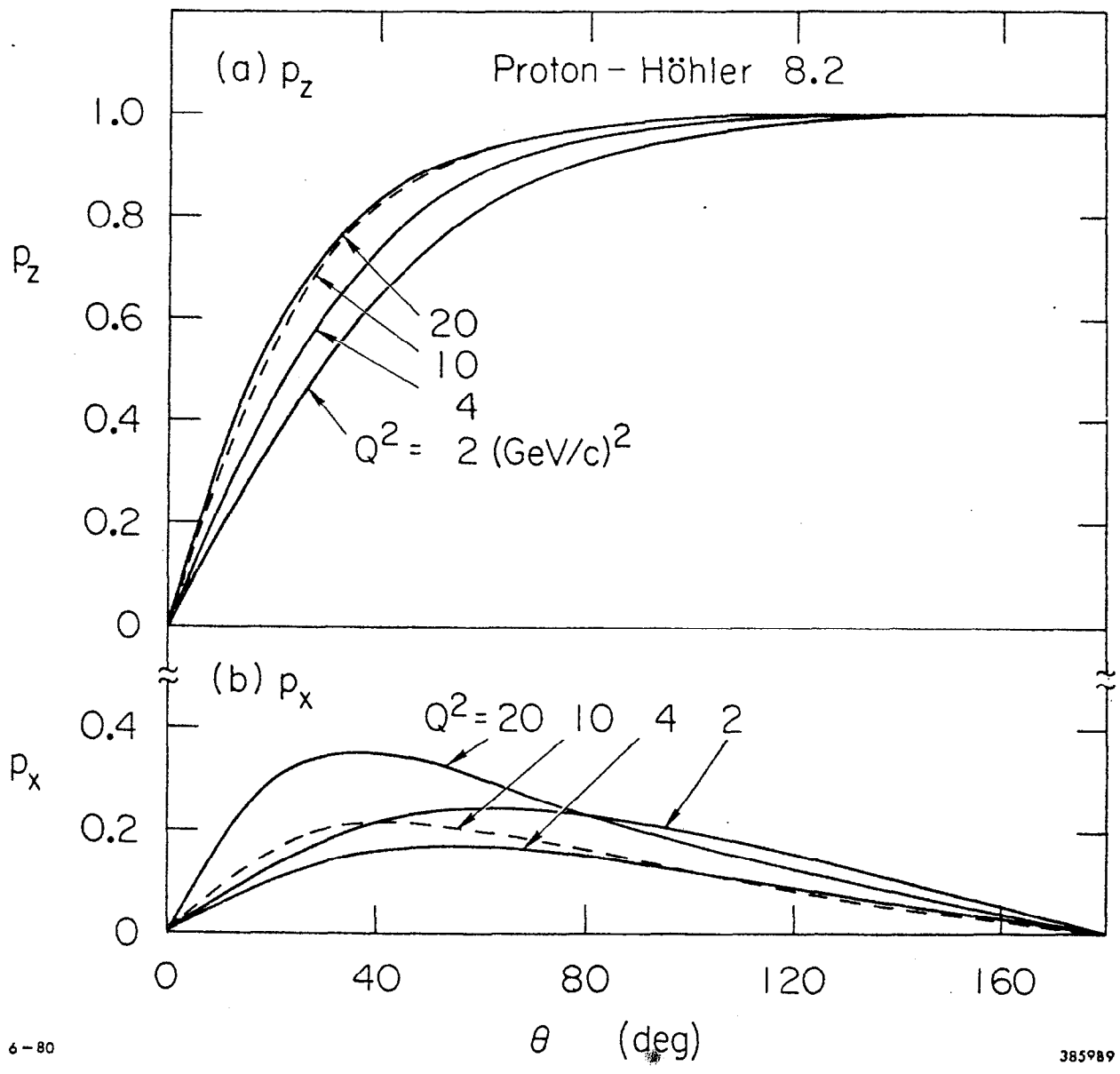


Fig. 9

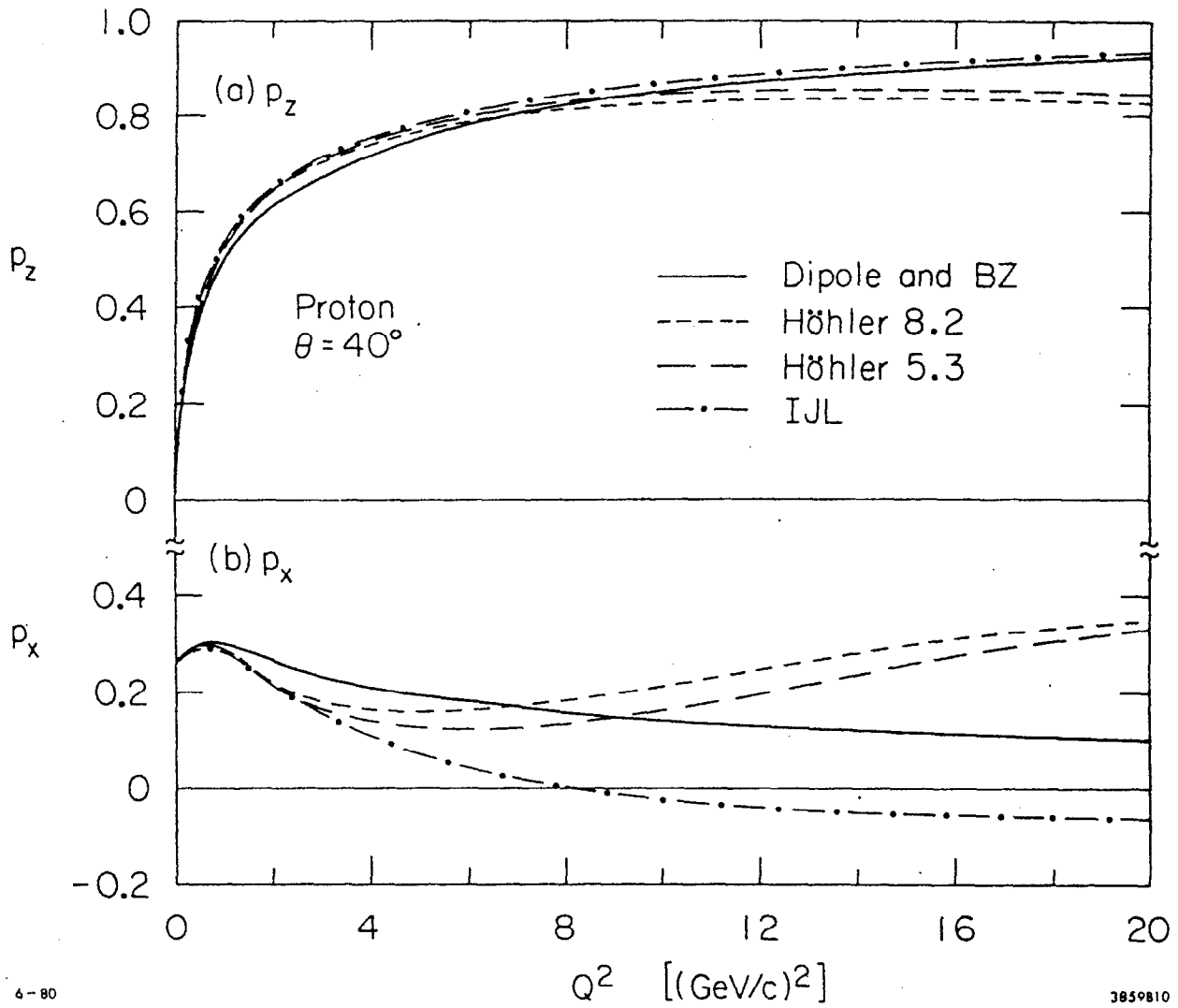


Fig. 10